ACS APPLIED MATERIALS & INTERFACES

www.acsami.org

Research Article

Actuation of Soft Thermoresponsive Hydrogels Mechanically Stimulates Osteogenesis in Human Mesenchymal Stem Cells without Biochemical Factors

Arturo Castro Nava, Iris C. Doolaar, Norina Labude-Weber, Hanna Malyaran, Susan Babu, Yashoda Chandorkar, Jacopo Di Russo, Sabine Neuss,* and Laura De Laporte*

Cite This: *ACS Appl. Mater. Interfaces* 2024, 16, 30−43

Read Online

ACCESS | Metrics & More | Article Recommendations | Supporting Information

ABSTRACT: Mesenchymal stem cells (MSCs) have the potential to differentiate into multiple lineages and can be harvested relatively easily from adults, making them a promising cell source for regenerative therapies. While it is well-known how to consistently differentiate MSCs into adipose, chondrogenic, and osteogenic lineages by treatment with biochemical factors, the number of studies exploring how to achieve this with mechanical signals is limited. A relatively unexplored area is the effect of cyclic forces on the MSC differentiation. Recently, our group developed a thermoresponsive *N*-ethyl acrylamide/*N*-isopropylacrylamide (NIPAM/NEAM) hydrogel supplemented with gold nanorods that are able to convert near-infrared light into heat. Using light pulses allows for local hydrogel collapse and swelling with physiologically relevant force and frequency. In this study, MSCs are cultured on this hydrogel system with a patterned surface and exposed to intermittent or continuous actuation of the hydrogel for 3 days to study the effect of actuation on MSC differentiation. First, cells are harvested from the bone marrow of three donors and tested for their MSC phenotype, meeting the following criteria: the harvested cells are adherent and demonstrate a fibroblast-like bipolar morphology. They lack the expression of CD34 and CD45 but do express CD73, CD90, and CD105. Additionally, their differentiation potential into adipogenic, chondrogenic, and osteogenic lineages is validated by the addition of standardized differentiation media. Next, MSCs are exposed to intermittent or continuous actuation, which leads to a significantly enhanced cell spreading compared to nonactuated cells. Moreover, actuation results in nuclear translocation of Runt-related transcription factor 2 and the Yes-associated protein. Together, these results indicate that cyclic mechanical stimulation on a soft, ridged substrate modulates the MSC fate commitment in the direction of osteogenesis.

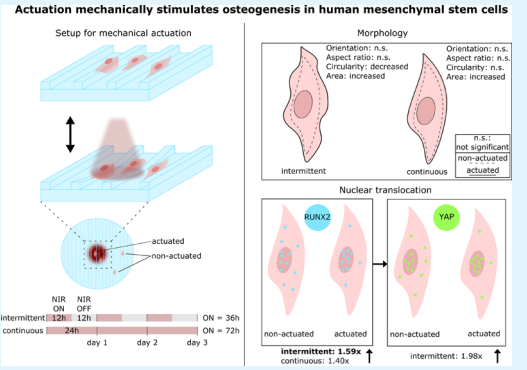

KEYWORDS: *mesenchymal stem cells, mechanotransduction, hydrogel, actuation, osteogenesis*

INTRODUCTION

Mesenchymal stem cells (MSCs) are multipotent stromal cells that have a high capacity for self-renewal and differentiation toward numerous mesodermal lineages.[1] MSCs exist in different adult tissues[2] and have been successfully isolated from various sources, such as bone marrow,[3] adipose tissue,[4] placenta,[5] and Wharton's Jelly of umbilical cords.[6] MSCs have been studied extensively because of their benefits related to supportive interactions with other cells, the production of bioactive factors, and the regulation of the immune system. For instance, MSCs create a suitable environment for hematopoietic stem cell differentiation,[7] show anti-inflammatory responses by modulating immune cell activity,[8] and inhibit the activation and cytotoxicity of resting natural killer cells.[9] In addition, they have beneficial effects on wound healing processes.[10] Another possible benefit of MSCs is their ability to not only differentiate along the mesodermal lineage[11] (e.g., adipocytes, chondrocytes, and osteoblasts) but also transdifferentiate into endodermal[12] and ectodermal layers.[13] However, these findings are controversial since they may be an artifact of in vitro culture systems and may not be relevant under physiological conditions in vivo.[1] For these reasons, controllable expansion and differentiation of MSCs is a prominent topic for cell-based therapies and tissue engineering.[14]

MSCs are classically grown, expanded, and differentiated in vitro on hard tissue culture polystyrene (TCPS) plates using

Received: August 9, 2023
Revised: November 2, 2023
Accepted: November 3, 2023
Published: December 27, 2023

complex cell culture media containing a variety of biochemical factors. These soluble molecules, such as growth factors, cytokines, amino acids, and other supplements, support cell growth and function, act as energy sources, and provide cues for cell development.[15]

However, in recent years, it has become apparent that not only biochemical but also mechanical signals can induce cell differentiation. In 2006, pioneering results showed that matrix elasticity has an effect on MSC differentiation. It was observed that very soft collagenous substrates (elastic modulus: 0.1−1 kPa) induce differentiation of MSCs into neuronal cells, whereas stiffer (8−17 kPa) and rigid (25−40 kPa) collagenous matrices favored myogenic and osteogenic differentiation, respectively.[16] Since then, numerous reports have further investigated the influence of mechanical and physical cues (stiffness, viscoelasticity, and topography) on stem cell fates in vitro.[17] For instance, MSCs cultured on soft polyacrylamide gels (250 Pa), which mimic the mechanical elasticity of the bone marrow, maintain a quiescent state while preserving their proliferation and differentiation potential.[18] More recently, the importance of stress relaxation on MSC differentiation was revealed, demonstrating that adipogenesis in soft hydrogels is reduced for rapidly relaxing gels, while osteogenesis is enhanced in stiffer, fast relaxing gels.[19] In fast relaxing gels, the cells demonstrated significantly more cell spreading. This effect is mediated through integrin binding and ligand clustering, affecting downstream actomyosin contractility and Yes-associated protein (YAP) nuclear translocation. Furthermore, another study showed that the critical stress value (threshold after which stress-stiffening occurs) can guide MSCs toward either adipogenesis or osteogenesis through involvement of DCAMKL1.[20] Here, lower critical stress (9.4−12.8 Pa) resulted in adipogenesis, while higher critical stress (14.6−19.3 Pa) led to osteogenesis in a soft hydrogel (storage modulus: 0.2−0.4 kPa). In addition to the stiffness, viscoelasticity, and strain-stiffening behavior of the substrate, micro- and nanoscale topographical features have also been proven to impact stem cell behavior. For example, MSCs differentiate toward adipocytes or osteoblasts, depending on the aspect ratio and curvature of geometric features. Adipogenesis is favored on islands with small areas (1000 μm^2) and lower aspect ratios, whereas osteogenic differentiation takes place on pillars with larger areas (5000 μm^2) and higher aspect ratios.[21] Generally, when MSCs are able to spread, YAP is shuttled to the nucleus, and osteogenesis is favored. In addition, osteogenic differentiation can be triggered by specific nanoscale topographies, such as TiO_2 nanotubular-shaped structures with a 70−100 nm diameter.[22] Thus, the geometry shape and size of material features regulate MSC commitment between those two lineages.[21,23]

As described above, local mechanostructural cues play an important role in stem cell function and fate. Nonetheless, cells in the human body are also constantly subjected to larger-scale internal stresses and cyclic strains. Therefore, material systems capable of mimicking the movement of the extracellular matrix (ECM) and tissue-dependent natural forces could provide answers to key mechanobiological questions. Systems that apply dynamic forces on cells have been engineered and fabricated to investigate how changing forces affect stem cell mechanotransduction and differentiation processes but often lack the ability to exert nativelike mechanical signals. The existing mechanical in vitro platforms range from macroscopic membranes or elastic surfaces that exert pure cyclic strain up to smart materials, which respond to user-defined stimuli (e.g., temperature, pH, light, and electric fields). Cyclic strain is most often applied by a polydimethylsiloxane (PDMS)-based system, which has been shown to enhance myogenic differentiation of MSCs cultured in myogenic medium[24] and increase mineral deposition of MSCs cultured in osteogenic medium.[25] Unfortunately, most of these materials and methods cannot provide relevant mechanical stresses to cells with precise user-defined localization.

In contrast, stimuli-responsive hydrogels better resemble the native ECM as their stiffness, viscoelasticity, biodegradation, and macromolecular properties can be fine-tuned.[26,27] For example, polyacrylamide hydrogel stiffness can be changed on demand upon addition of a soluble linker DNA strand or a release strand. The hydrogel with oligonucleotide-based cross-links can then be reversibly stiffened or softened, respectively.[28,29] In addition, a light stimulus can be applied to stiffen or soften the hydrogel, for example, by changing cyanobacterial phytochrome 1 from the monomeric state to a dimeric state by switching from 740 to 660 nm light,[30] or by UV-assisted cleavage of photodegradable poly(ethylene glycol) (PEG),[31] respectively. The use of the photodegradable PEG hydrogel revealed that MSCs have a mechanical memory, driven by YAP/TAZ activation, that affects their differentiation potential.[32] This system enables studying MSC behavior in stiff-to-soft changing regimes in a controlled manner, altering the elastic modulus from 10 to 2 kPa. This softening takes around 6 min, but the change in stiffness is not reversible.

Therefore, we previously reported a mechanically reversible, dynamic hydrogel platform with variable microtopographies in order to tune (sub)cellular mechanical forces on cells.[33] The platform consists of a thermoresponsive cross-linked hydrogel prepared from a 60/40 ratio of *N*-isopropylacrylamide (NIPAM) and *N*-ethyl acrylamide (NEAM) to obtain a volume phase transition temperature (VPTT) of approximately 37 °C. Gold nanorods (AuNRs) are incorporated to convert near-infrared (NIR) light to heat and locally collapse the hydrogels. By exposure to laser pulses, the hydrogel can be actuated at a precise location with a defined amplitude and frequency of up to 10 Hz. We demonstrated that fibroblasts become less mobile when actuated, with enhanced focal adhesions and ECM production, while myocardin-related transcription factor A (MRTFA) shuttles to the nucleus.[33] Furthermore, in myoblasts, the actuation enhances proliferation and migration, while myogenic factors such as MyoD and YAP translocate in the nucleus promoting myogenesis,[34] suggesting that the response to mechanical stimulation is different for different cell types.

In this study, we show that MSCs exhibit changes in their morphology and cellular spatial organization upon mechanical actuation. Furthermore, the applied forces, depending on the actuation parameters set, trigger preosteoblastic MSC differentiation in basal medium without differentiation factors after actuation for 3 days. This is shown by the translocation of Runt-related transcription factor 2 (Runx2) and YAP after actuation. Therefore, this light-responsive dynamic hydrogel system gives first insights into the effect of dynamic actuation on a soft hydrogel substrate on human MSC differentiation in the absence of biochemical differentiation factors.

MATERIAL AND METHODS

Hydrogel Preparation. Patterned NIPAM/NEAM hydrogels with a VPTT of 37 °C and an elastic modulus of ∼30 kPa at 36 °C are

https://doi.org/10.1021/acsami.3c11808
ACS Appl. Mater. Interfaces 2024, 16, 30−43

fabricated according to the methods described previously.[33] Briefly, hydrogels are fabricated by copolymerization of a 0.2 g of NIPAM and 0.12 g of NEAM (molar ratio: 60/40, both Sigma-Aldrich) precursor solution containing 3.6 AuNRs/μm^3 (AuNRs produced like described before[33]), 333 μL of DMSO (Sigma-Aldrich), 6.6 mg of photoinitiator (Irgacure 2959, Sigma-Aldrich), and 4.5 mg of cross-linker (*N*,*N*′-methylenebis(acrylamide), Sigma-Aldrich). Patterned hydrogels with continuous ridges (25 μm wide, 2.7 μm high) and grooves (25 μm wide) are obtained by casting the polymer solution on an etched, custom-made silicon wafer with the inverse predefined geometry (25 μm wide ridges and grooves, 2.7 μm height). These dimensions are used since they avoid crease formation due to mechanical buckling of the gel and are in the range of the dimensions of a cell (~20 μm), and ridge deformation is predominant in the lateral direction as compared to the axial direction.[33] Then, hydrogels are cured under UV light (Konrad Benda lamp, 366 and 254 nm, 8 W), washed with deionized water and then Milli-Q water, and finally sterilized in 70% ethanol (Sigma-Aldrich). To facilitate cell adhesion, the surface of the hydrogels (Ø 9 mm) is covalently functionalized with fibronectin (Sigma-Aldrich) using sulfosuccinimidyl 6-(4′-azido-2′-nitrophenylamino)hexanoate (Sulfo-SANPAH, Thermo Fischer) as a covalent linker. Sulfo-SANPAH (3.38 mM, 20 μL per gel) is added on top of the gel and activated by UV illumination (UV Hand Lamp 254 and 365 nm 8 W tube, Herolab) for 14 min. The gel is then washed 3 times with Milli-Q, after which Fibronectin (265 nM, 15 μL per gel) is added to the gel and allowed to incubate overnight at 32 °C. Nonbound fibronectin is removed by washing with Milli-Q 3 times.

Cell Culture. Human mesenchymal stem cells (MSCs) are isolated and cultured according to protocols from Haynesworth et al.[35] and Pittenger et al.[11] and in the same way we have described previously.[36] In brief, MSCs are isolated from surgically removed femoral heads of patients with total hip endoprosthesis, provided by the Orthopedic Clinics of the University Hospital RWTH Aachen University. Experiments are performed with informed consent of the affected patients and are approved by the local Ethics Committee (EK 187/08). After isolation, the MSCs are expanded in stem cell culture medium (SCM) (Mesenpan, PanBiotech), which is changed every 3−4 days. MSCs from passages 1 to 3 are used for the experiments. In contrast to the previously described protocol, cells are centrifuged at 500*g* instead of 250*g*.

Differentiation Assays on Tissue Culture Polystyrene. Primary MSCs are differentiated toward other lineages in order to demonstrate their in vitro differentiation potential into osteocytes, chondrocytes, and adipocytes under appropriate cell culture conditions. MSCs undergo multipotent differentiation on TCPS while exposed to media supplemented with specific differentiation inducing biochemical factors, while control cells are cultured in SCM, which does not contain those factors.

For adipogenic differentiation, MSCs are seeded with a density of 80,000 cells/cm^2 in SCM. On the next day, SCM is changed to adipogenic induction medium (AIM), consisting of DMEM high glucose (4.5 g/L glucose) (Gibco), supplemented with 10% FCS (PAN-Biotech), 1 μM dexamethasone (Sigma-Aldrich), 0.2 μM indomethacin (Sigma-Aldrich), 0.5 mM IBMX (Sigma-Aldrich), 0.01 mg/mL human Insulin (Sigma-Aldrich), and 1% LGPS (80 U/mL Penicillin; 80 μg/mL streptomycin; 1.6 mM L-glutamine) (Gibco). Medium is exchanged every 2 days, alternating with adipogenic maintenance medium (AMM) made of DMEM high glucose (4.5 g/L glucose) (Gibco), supplemented with 10% FCS (PAN-Biotech), 0.01 mg/mL human insulin (Sigma-Aldrich), and 1% LGPS (80 U/mL Penicillin; 80 μg/mL Streptomycin; 1.6 mM L-glutamine) (Gibco). After 7, 14, and 21 days of adipogenic differentiation, cells are fixed in 50% ice-cold ethanol for 30 min and further analyzed by Oil red O staining (Sigma-Aldrich) to determine the formation of lipid droplets. Cell nuclei are counterstained with Hemalum (Sigma-Aldrich).

For chondrogenic differentiation, 250,000 cells are initially cultured as pellet cultures in SCM in 15 mL tubes. One day after seeding, SCM is changed to chondrogenic induction medium (CIM) consisting of DMEM high glucose (4.5 g/L glucose) (Gibco), 100 nM dexamethasone (Sigma-Aldrich), 0.17 mM L-ascorbic-acid-2-phosphate (Sigma-Aldrich), 100 μg/mL sodium pyruvate (Sigma-Aldrich), 4 μg/mL L-proline (Sigma-Aldrich), 10 ng/mL TGF-β_3 (R&D Systems), 1% LGPS (80 U/mL Penicillin; 80 μg/mL streptomycin; 1.6 mM L-glutamine) (Gibco), and 5 mL ITS-Plus Premix (6.25 μg/mL bovine insulin; 6.25 μg/mL transferrin, 6.25 μg/mL selenium acid, 6.25 μg/mL linoleic acid, and 6.25 μg/mL BSA) (Life Technologies). It is important to mention that TGF-β_3 is always added freshly to the medium (0.5 μL/mL medium). Medium is exchanged three times a week. After days 7, 14, and 21 of chondrogenic differentiation, cells form pellets that are fixed in 4% formalin (Morphisto) overnight, dehydrated, embedded in paraffin (Sigma-Aldrich), and sectioned into 2−3 μm thick slices. Afterward, cell pellets are stained with Toluidine blue (Sigma-Aldrich) to visualize glycosaminoglycan deposition.

For osteogenic differentiation, MSCs are cultured with a density of 31,000 cells/cm^2 in SCM, based on previous studies.[37] This medium is exchanged the next day to osteogenic induction medium (OIM) consisting of DMEM low glucose (1 g/L glucose) (Gibco), 10% FCS (PAN-Biotech), 100 nM dexamethasone (Sigma-Aldrich), 10 mM sodium-β-glycerophosphate (Sigma-Aldrich), 0.05 mM L-ascorbic-Acid-2-phosphate (Sigma-Aldrich), and 1% LGPS (80 U/mL penicillin; 80 μg/mL streptomycin; 1.6 mM L-Glutamine) (Gibco). Medium exchange is done three times per week. After 7, 14, and 21 days, cells are fixed in ice-cold 70% ethanol, and calcium depositions are determined by Alizarin Red (Sigma-Aldrich) staining.

Immunophenotype Analysis. The surface epitopes of the MSCs are analyzed by flow cytometry. Briefly, MSCs are trypsinized, counted, and kept in flow cytometry buffer (0.09% FCS in PBS (Gibco)). Cells are centrifuged at 500*g* for 5 min at 4 °C and then resuspended in 100 μL of flow cytometry buffer with the antibodies. The APC-, PE-, or FITC-isotype controls and conjugated antibodies against CD34, CD45, CD73, CD90, and CD105 (eBioscience) are diluted 1:500. Then, cells are incubated for 30 min at 4 °C and centrifuged, and the supernatant is removed. Finally, cells are resuspended in 200 μL of flow cytometry buffer. Immunophenotype analysis is done with a FACS Canto II cytometer (BD Bioscience), and at least 10,000 events are measured for each MSC donor.

Cell Actuation. MSCs are seeded with a density of 10,000 cells/cm^2 in 0.5 mL of SCM on the gels (Ø 9 mm) and are left undisturbed for the next 4 h inside a cell culture incubator at 37 °C, 5% CO_2, and 95% humidity. Afterward, SCM is exchanged to basal medium made of DMEM low glucose (1 g/L glucose) (Gibco), 1% FCS (PAN-Biotech), and 1% PS (80 U/mL penicillin; 80 μg/mL streptomycin) (Gibco). Hydrogels are immediately placed in the custom-made laser actuation setup acquired from AIQTEC LTD, as previously described,[33] where a defined region of the hydrogel is mechanically actuated with the NIR laser using the experimental parameters shown below (Tables 1, 2, and Movie S1). MSCs that are at least 300 μm away from the actuated area are randomly selected as nonactuated cells. These cells have been exposed to all the same conditions (e.g., hydrogel and coating, passage number, seeding density, and environmental conditions) except actuation, which makes them a good control population. Note that it was previously shown that cells on the same gel did not alter their behavior.[33] For further analysis, no distinct selection was made for cells in grooves or on ridges.

Table 1. Exposure Parameters for Intermittent and Continuous Actuation

	laser exposure/day (h)	rest time/day (h)	total time of actuation (h)	total time of experiment (h)
intermittent actuation	12	12	36	72
continuous actuation	24	0	72	72

Immunostaining and Microscopy. Immediately after the actuation experiment, the samples are rinsed twice with PBS, fixed

https://doi.org/10.1021/acsami.3c11808
ACS Appl. Mater. Interfaces 2024, 16, 30−43

Table 2. Laser Settings

laser power (mW)	time ON (ms)	time OFF (ms)	frequency (Hz)	actuation amplitude (μm)[a]	relative displacement (%)[a]	estimated force (nN)[a]
340	100	1900	0.5	4.35	14	141.91

[a]Measured/calculated previously.[33]

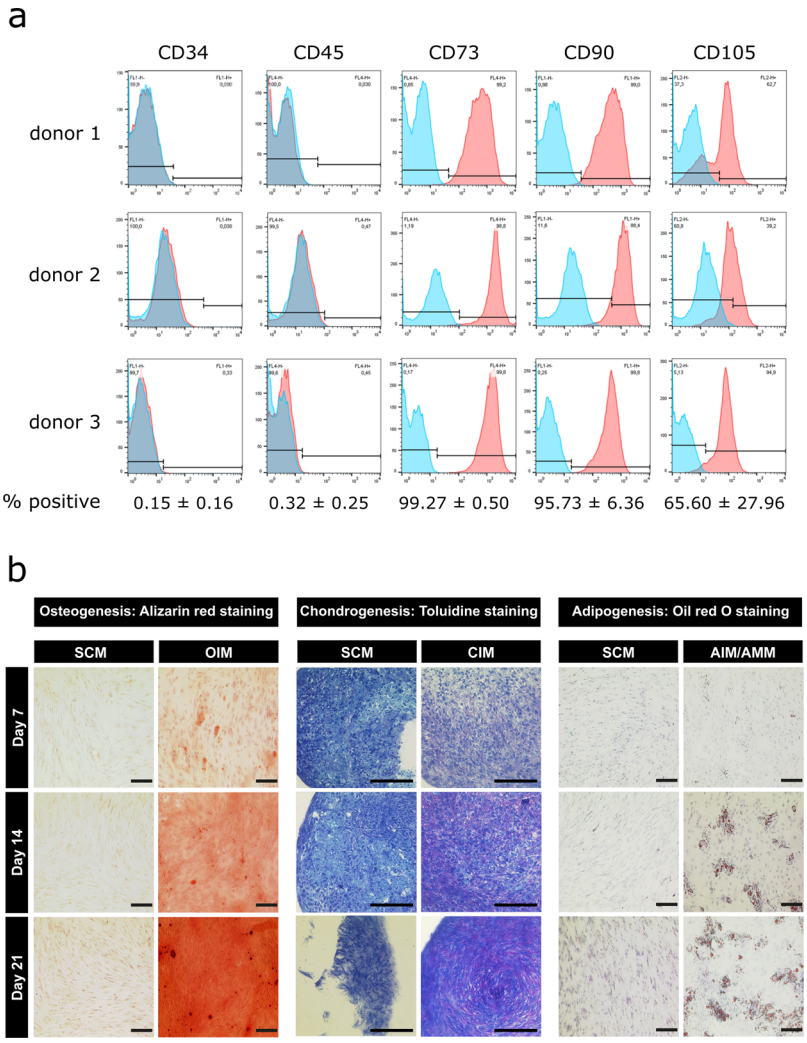

Figure 1. Cells harvested from all three donors can be defined as mesenchymal stem cells according to the criteria from the International Society for Cellular Therapy (ISCT). (a) Harvested cells are negative for surface markers CD34 and CD45 and positive for CD73, CD90, and CD105. Representative histograms of the immune phenotype analysis of three MSC donors at passages 1−3. MSCs are labeled with antibodies against specific antigens and further analyzed by flow cytometry. The blue curves indicate the fluorescence of isotype controls, while the red curves show the fluorescence of the MSCs stained against specific antibodies. The figure also shows the percentage of MSCs with positive surface epitope expression. (b) Harvested cells show differentiation potential for osteogenic, chondrogenic, and adipogenic lineages on TCPS when treated with specific induction media. Representative images of MSCs from one donor differentiated into osteogenic, chondrogenic, and adipogenic lineages, as shown by histological stainings which are performed after 7, 14, and 21 days of cell culture. n = 3 donors. Scale bar = 200 μm. AIM: adipogenic induction medium, AMM: adipogenic maintenance medium, CIM: chondrogenic induction medium, MSC: mesenchymal stem cell, OIM: osteogenic induction medium, SCM: stem cell culture medium, TCPS: tissue culture polystyrene.

with 4% paraformaldehyde (AppliChem) for 30 min, and washed thrice with PBS. Cells are then permeabilized with 0.1% Triton X (Sigma-Aldrich) for 8 min before three additional washing steps with PBS. Samples are then incubated for 1 h with 3% BSA (Sigma-Aldrich) in PBS to block nonspecific bindings followed by the addition of primary antibodies against Runx2 (NovusBiologicals, NBP1−77462) or YAP (Santa Cruz Biotechnology, sc-101199) using a dilution of 1:100. Samples are incubated for 4 h at room temperature before being rinsed three times with PBS. Afterward, samples are incubated for 1 h at room temperature with the secondary antibodies antirabbit Alexa Fluor 633 (Thermo Fischer, A-21071) or antimouse Alexa Fluor 488 (Thermo Fischer, A32723) using a dilution of 1:200. Cells are then washed three times with PBS, after which cell nuclei are counterstained with DAPI (4′,6-diamidino-2-phenylindole) for 8 min at room temperature with a dilution of 1:100. Finally, samples are washed three times with PBS and stored at 4 °C for further analysis.

Confocal laser scanning microscopy is performed with a Leica SP8 Tandem Confocal system equipped with a white light laser and a heating chamber set at 37 °C. Samples are excited with the suitable wavelengths, and light emission from DAPI or Runx2 and YAP is detected with photomultiplier tubes or hybrid detectors, respectively. These detectors are set in counting mode when Runx2 or YAP is being imaged, and sequential scanning is used while imaging.

https://doi.org/10.1021/acsami.3c11808
ACS Appl. Mater. Interfaces 2024, 16, 30−43

Confocal images are imported to ImageJ (Fiji, version 1.52p) to determine morphological parameters and quantify nuclear and cytoplasmic Runx2 and YAP. To separate the cytoplasm and nucleus, the same protocol as the one described previously is used.[33] Briefly, orthogonal maximum intensity projections are first created from the Z-stack. Then, the DAPI and, instead of actin, Runx2 or YAP channels from the image are used to obtain the mask for the nucleus and cytoplasm via Otsu's thresholding method. Boolean operators (SUBSTRACT and AND) and the DAPI mask are then used to separate images containing a nuclear or cytoplasmic fluorescent signal.

The traced cell outline is then used to determine the cell area and generate a best-fit ellipse from which the mean orientation angle, aspect ratio, and circularity could be determined. The area and orientation angle are given by the Fiji parameters "Area" and "Angle", respectively. The orientation angle is then subtracted by 90° to obtain the orientation angle from the axis of the patterned lines of the hydrogel (which were vertical). For the aspect ratio and circularity, the following formulas are used:

$$\text{Aspect ratio} = \frac{\text{major axis length}}{\text{minor axis length}}$$

$$\text{Circularity} = \frac{4\pi \cdot \text{Area}}{\text{Perimeter}^2}$$

The major and minor axis length are given by the Fiji parameters "Major" and "Minor", whereas the perimeter is given by 'Perim.'

In order to determine the fluorescence intensity from Runx2 or YAP, a circular region of interest with an area of 3 μm^2 is placed in three random regions within the cell nucleus and cytoplasm of the raw fluorescence images, and the average fluorescence intensity of these areas is determined. Data are plotted as the mean fluorescence intensity of nuclear to cytoplasmic signal ratio in actuated and nonactuated samples. For Runx2, $N \geq 115$ cells are analyzed from three independent experiments; while for YAP, results from $N \geq 95$ cells are quantified from two independent experiments.

Statistical Analysis. Data and statistical analyses are performed using OriginPro 2016G (b9.32.303) software. All data are shown as mean ± standard deviation, unless specified otherwise. After performing a normality test (Shapiro–Wilk, significance level 0.05) and a two-sample test for variance (significance level 0.05) for each experiment, normality and equal variance could not be assumed. Therefore, statistical significance is determined by a Mann–Whitney test defined at $p < 0.05$, 0.01, and 0.001, represented by *, **, and *** respectively.

RESULTS

Harvested Cells Are Identified as MSCs. Cells harvested from the bone marrow of three donors are subjected to the criteria of the Mesenchymal and Tissue Stem Cell Committee of the International Society for Cellular Therapy (ISCT) to validate their MSC identity. First, we observed that the harvested cells are adherent and demonstrate a fibroblast-like, bipolar morphology.

Surface Epitope Characterization. Second, different cell-surface epitopes are evaluated by flow cytometry analysis. The forward and side scatter density plot and gate are provided in Figure S1. Harvested cells from all three donors lack expression of CD34 (<1% positive) and CD45 (<1% positive), while all MSCs express CD73 (>95% positive), CD90 (>95% positive), and CD105 (>65% positive) [Figure 1a]. These results comply with the first criterion of the MSC identity.

An additional flow cytometry experiment is performed where MSCs are cultured on either TCPS or on the hydrogels for 3 days without actuation. They are kept in either SCM, basal medium, or OIM. Expression of cell-surface epitopes did not change over 3 days of culture time, between SCM or basal medium and between the two substrates (Table 3); thus, it can be assumed that further cellular changes will be caused by the actuation.

Table 3. Average Expression of Cell-Surface Epitopes on MSCs from All Three Donors Based on Flow Cytometry Measurements after Culture on Different Substrates in Different Media for 3 Days[a]

	hydrogels		
	SCM	basal medium	OIM
CD34	0.06 ± 0.03	0.13 ± 0.18	32.71 ± 56.54
CD73	98.00 ± 1.47	98.20 ± 1.41	65.11 ± 56.10
CD45	0.17 ± 0.09	0.10 ± 0.05	0.18 ± 0.15
CD90	95.97 ± 2.41	97.17 ± 2.16	96.00 ± 1.91
CD105	89.70 ± 7.63	92.23 ± 5.83	90.47 ± 7.27
	Tissue culture plastic		
	SCM	basal medium	OIM
CD34	0.06 ± 0.07	0.14 ± 0.21	0.13 ± 0.18
CD73	98.10 ± 1.44	98.47 ± 0.90	98.57 ± 1.00
CD45	0.19 ± 0.24	0.08 ± 0.10	0.21 ± 0.16
CD90	96.20 ± 2.55	97.37 ± 1.90	96.60 ± 2.51
CD105	92.33 ± 4.08	92.67 ± 2.14	93.67 ± 5.20

[a]SCM: stem cell culture medium, OIM: osteogenic induction medium.

MSC Differentiation on TCPS. The third criterion is the ability to differentiate between osteogenic, chondrogenic, and adipogenic lineages using standardized induction cell culture media supplemented with the required differentiation factors for each lineage. Osteogenic differentiation is promoted by using the OIM, which is confirmed by the Alizarin red staining. This stain can be used to identify calcium phosphate deposits, an important component of bone. MSCs treated with the OIM display these extracellular calcium accumulations (visible in red) already at day 7, which are gradually increased until day 21. This effect is not visible for MSCs cultured with SCM (Figure 1b). Chondrogenic differentiation is achieved by culturing MSCs with a CIM. This is validated by using toluidine blue, which stains collagen, proteoglycans, and glycosaminoglycans within the ECM. Samples cultured with CIM reveal vast amounts of ECM components, as shown by the dark blue staining and they are hyaline in appearance (purple), unlike control samples, which have a lighter blue color and no hyaline formation [Figure 1b]. Adipogenic differentiation is induced in MSCs by the addition of AIM and AMM. Adipose differentiation is validated by confirming the formation of fat droplets and lipid vacuoles with Oil red O staining, which colors fats red. Samples grown with adipogenic induction medium/adipogenic maintenance medium (AIM/AMM) show small clusters of lipid droplets at day 7, while larger and filled vacuoles are observed at later time points. By comparison, MSCs cultured with SCM show no lipid formation [Figure 1b]. Images from differentiation experiments for the other two donors (donors 1 and 3) are shown in Figure S2. From these results, combined with the validation of the expression of the correct surface epitopes, we can conclude that the harvested cells can be identified as MSCs.

Mechanical Actuation Affects MSC Morphology. To first determine whether dynamic mechanical forces alter morphological features of MSCs, stem cells are seeded on fibronectin-coated patterned 60/40 NIPAM/NEAM hydrogels (elastic modulus of ∼30 kPa) (Figure 2). A ridge-groove

https://doi.org/10.1021/acsami.3c11808
ACS Appl. Mater. Interfaces 2024, 16, 30−43

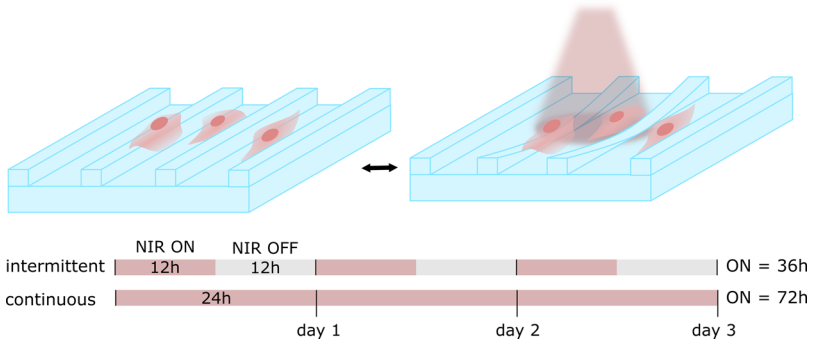

Figure 2. Overview of the actuating hydrogel setup.

pattern is used as it avoids crease formation due to mechanical buckling of the gel, and deformation of the ridge is predominant in the lateral direction as compared to the axial direction.[33] During actuation, the gels are locally exposed to NIR light, and the gold nanorods that are incorporated into the gels will transform the NIR light into heat, causing the gel to locally collapse. We would like to point out that the used duty cycles/laser ON time (100 ms) and the presence of the large heat sink lead to a rapid thermal equilibrium, while the temperature of the medium and nonirradiated portion of the gel does not increase.[33] It was also previously shown that the mean local temperature is only slightly increasing (fluctuation of ∼0.3 °C around a new equilibrium that is ∼0.6 °C higher than before irradiation) for an ON-time of 100 ms and frequency of 1 Hz. During hydrogel actuation, the local temperature, stiffness, and hydrophobicity, therefore, only marginally change back and forth at a high frequency, while the cells are in direct contact with a covalently linked fibronectin coating on top of the hydrogels. In that report, we also demonstrated that the actuated cells do not express more Hsp 70 or Elf (which stains stress granules and P-bodies, both are markers for phototoxic stress) than the nonactuated cells (L929 fibroblasts) and that the cells are not affected by the exposure to NIR light or the local temperature changes if no actuation takes place.[33] Because of the purpose of this study, MSCs are cultured in DMEM basal medium in order to avoid any biochemical factors that could directly inhibit or induce stem cell maintenance or differentiation. MSCs are allowed to adhere to the hydrogel at least 4 h before being subjected to intermittent (12 h actuation/12 h rest for 3 days) or continuous stimulation (24 h actuation per day for 3 days) using NIR light pulses (340 mW, 0.5 Hz, 100 ms ON time). We note that the actuation is completely reversible, so even after 3 days, the gel goes back to its original shape and dimensions when the laser is turned off. In earlier reports using this light-actuating hydrogel system with fibroblasts or myoblasts, a frequency of 1 Hz was used.[33,34] For the MSCs, the laser frequency is adjusted to a lower frequency of 0.5 Hz as low viability was observed at 1 Hz (data not shown). For the duration of actuation, we selected 3 days, as this is enough time to see an early osteogenic response (YAP and Runx2) and was used before in other similar studies.[38] Previous studies have also shown that cells can react differently to continuous versus intermittent stretch. For example, continuously stretched MSCs can be overstimulated, hindering chondrogenesis, whereas this is not the case for intermittently stretched MSCs.[39] Therefore, we include an intermittent condition (with cycles of 12 h on and 12 h off), as we previously saw the highest effect of actuation on MRTFA shuttling after 12 and 24 h in L929 fibroblasts.[33] Additionally, another similar study with MSCs found elevated mRNA levels of Runx2 at 6 and 12 h.[38]

Briefly, MSCs are cultured on NIPAM/NEAM hydrogels with parallel ridges (width: 25 μm, height: 2.7 μm) and grooves (width: 25 μm). Due to the photothermal effect of the gold nanorods that are incorporated into the hydrogels, the gel heats up when irradiated with a NIR laser, causing the hydrogel to collapse. When the laser is off, the gel quickly returns to the normal swollen state. Actuation is therefore achieved with a laser pulse of 0.5 Hz (100 ms ON, 1900 ms OFF), and cells are exposed to 3 days of either 12 h of actuation and 12 h of rest or 24 h of actuation.

After 3 days in culture, MSCs grown in all conditions sense and follow the underlying topographic cues (Figure 3a−c). The mean orientation angle θ (defined as the angle between the main axis of the cell and a line parallel to the ridges) for the cytoplasm (θ_{cyt}) and nucleus (θ_{nuc}) in both conditions has a value between $-1.6° < \theta_{cyt} < 1.8°$ and $-2.8° < \theta_{nuc} < 1.0°$, respectively (Figure 3b,c). Thus, cellular directionality is induced along the parallel-patterned hydrogel. Hydrogel actuation does not have a significant effect on cellular or nuclear orientation, compared to static conditions, and thus this type of mechanical stress does not change cellular direction.

Besides MSC orientation along the lined pattern, the hydrogel topography can affect cellular elongation, measured by cellular aspect ratios, and enhance differentiation.[40] However, both cytoplasmic ($5.8 < AR_{cyt} < 8.0$) and nuclear ($AR_{nuc} \sim 1.5$) aspect ratios (defined as the ratio of the major to the minor axis of the best fitting ellipse) remain unaffected in the presence of mechanical strain [Figure 3d,e]. Such cellular elongation along the underlying structures can be further correlated by the circularity parameter (C), which indicates whether a particular structure can be described as a circle (1.0) or an elongated shape (∼0.0). Irregular perimeters will also further decrease the circularity parameter. Therefore, this gives us information about how well cells spread in all directions. In general, the cytoskeleton stretches out parallel to the ridges and grooves ($C_{cyt} \sim 0.1$), while the nuclear parameter exhibits a more rounded shape ($C_{nuc} \sim 0.7$) [Figure 3a,f,g]. These results support the ones obtained for the aspect ratio, which is lower for the nucleus than for the cell. Nonetheless, by taking a closer look at the individual values for both conditions, it is observed that C_{cyt} decreases upon intermittent mechanical actuation, whereas this effect does not take place for continuous actuation periods. The quantitative results for the intermittent condition show that C_{cyt} decreases 1.54-fold (p =

https://doi.org/10.1021/acsami.3c11808
ACS Appl. Mater. Interfaces 2024, 16, 30−43

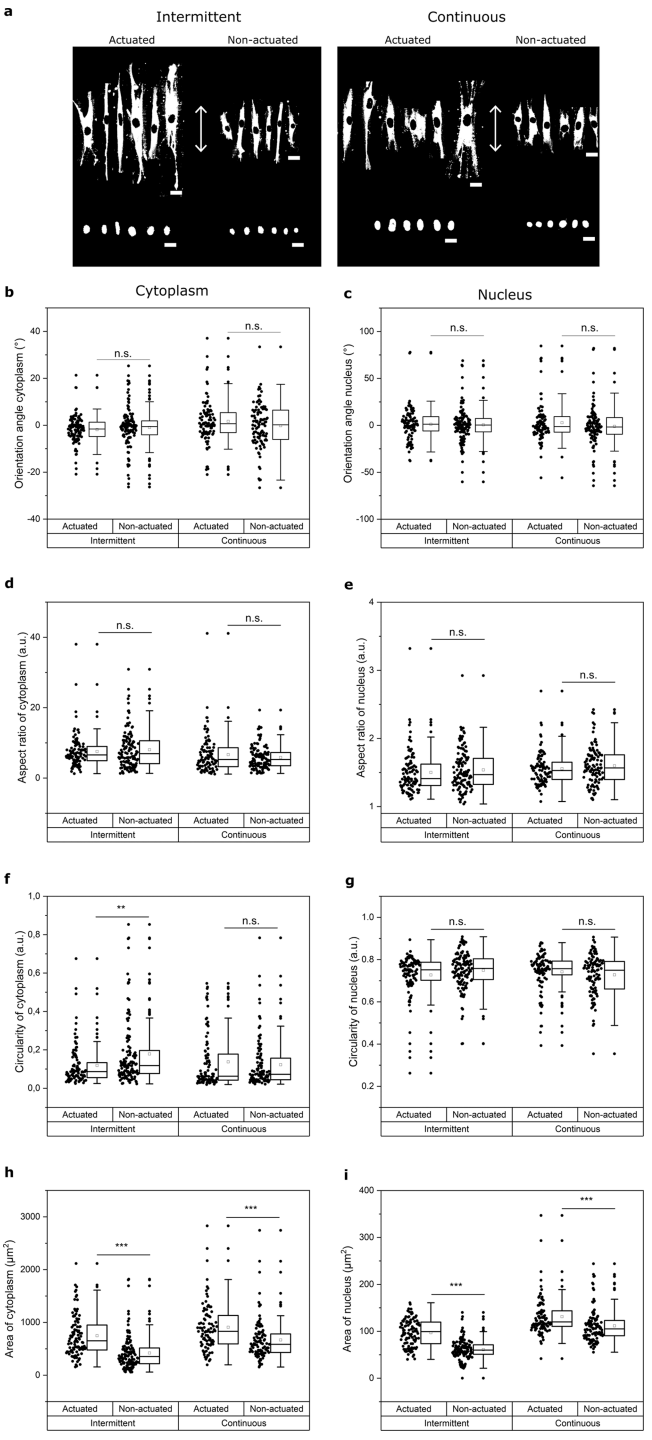

Figure 3. MSCs on patterned NIPAM/NEAM hydrogels change their cytoplasmic/nuclear morphology when exposed to intermittent or continuous actuation compared with no actuation. (a) Cytoplasmic and nuclear outlines of MSCs exposed to intermittent, continuous, or no actuation for 72 h. The arrows show the direction of the underlying patterned topography. Scale bar = 20 μm. (b–i) Actuation affects several morphological parameters of the cell and nucleus. Morphological parameters are the (b, c) orientation along the substrate pattern, (d, e) elongation, (f, g) circularity, and (h, i) spreading area. For the cytoplasm, the circularity was greater in intermittently actuated cells. For both cytoplasm and nucleus, the area was greater after both intermittent and continuous actuation compared to nonactuated cells. In all cases, the box plots show data from all 3 donors, with $N \geq 90$ cells in total. In the box plots, the interquartile range (IQR) between the first and the third quartiles is indicated by the box, while whiskers denote 1.5 IQR. The hollow square, the horizontal line, and the filled dots represent the average, the median, and the outliers, respectively. *, **, and *** are determined using a Mann–Whitney test and represent statistical significance at $p < 0.05$, 0.01, and 0.001, respectively. MSC: mesenchymal stem cell, NIPAM: *N*-isopropyl acrylamide, NEAM: *N*-ethyl acrylamide.

0.001) compared to nonactuated conditions [Figure 3 f,g]. The circularity of the nucleus did not significantly change with either intermittent or continuous actuation, which could be due to the stiffer character of the nucleus compared to the cytoplasm of the cell.[41] As the aspect ratio does not alter due to actuation, this is an indication that cells may be spreading more and hence have a more irregular morphology after being subjected to mechanical stress compared with cells that remain in static regions of the hydrogel.

In addition to the orientation, elongation, and circularity, cellular spreading areas of actuated and nonactuated cells are analyzed [Figure 3h,i]. From the MSC cytoplasmic and nuclear outlines [Figure 3a], it is clear that mechanically stimulated MSCs show a significant increase in cytoplasmic and nuclear areas in both actuating conditions. Quantitative analysis of cellular spreading area indicates that the mean cytoplasmic area increases 1.78-fold in the case of intermittently actuated cells versus nonactuated cells, whereas this area increases 1.35-fold in the continuous condition. For the nuclear area, the values are 1.58- (intermittent) and 1.17-fold (continuous) higher compared to nonactuated cells. These results exhibit how MSC spreading highly depends on dynamic forces exerted by soft hydrogels.

Cyclic Mechanical Actuation Induces Preosteoblastic Differentiation in MSCs. *Cyclic Mechanical Actuation Induces Runx2 Nuclear Translocation.* Previous studies have provided evidence that large MSC spreading areas, as often observed when these cells are cultured on high stiffness substrates, are linked to osteogenic differentiation.[42] After observing the significant increase in the cellular spreading area upon mechanical actuation, we continued by investigating the role of dynamic hydrogel actuation in initiating osteogenesis. Runx2 has been identified as the 'master osteogenic transcription factor,' which is activated through TGF-β_1 and BMP pathways.[43] When activated, Runx2 translocates to the nucleus, where it binds to the DNA. Therefore, the activity of Runx2 can be analyzed by the fluorescence intensity of the nuclear to cytoplasmic signal ratio of Runx2 ($Runx2_{nucleus}/Runx2_{cytoplasm}$). As Runx2 is an essential transcription factor expressed in early osteoblastic progenitors within the nucleus,[44] it is compared for actuated and nonactuated MSCs.

Based on immunofluorescence images [Figure 4a,b], MSCs exposed to cyclic mechanical forces visibly exhibit a predominant Runx2 signal in the nucleus compared to the cytoplasm. Moreover, quantitative analysis of this early osteogenic protein shows that the average fluorescence intensity ratio of $Runx2_{nucleus}/Runx2_{cytoplasm}$ is increased 1.59-fold in MSCs subjected to intermittent mechanical forces, whereas continuously stimulated MSCs show a 1.40-fold increase when compared to nonstimulated cells [Figure 4c].

Cyclic Mechanical Actuation Induces YAP Nuclear Activation and Localization. As nuclear Runx2 and YAP localization are sensitive to cell spreading,[19,45] we expect that

https://doi.org/10.1021/acsami.3c11808
ACS Appl. Mater. Interfaces 2024, 16, 30–43

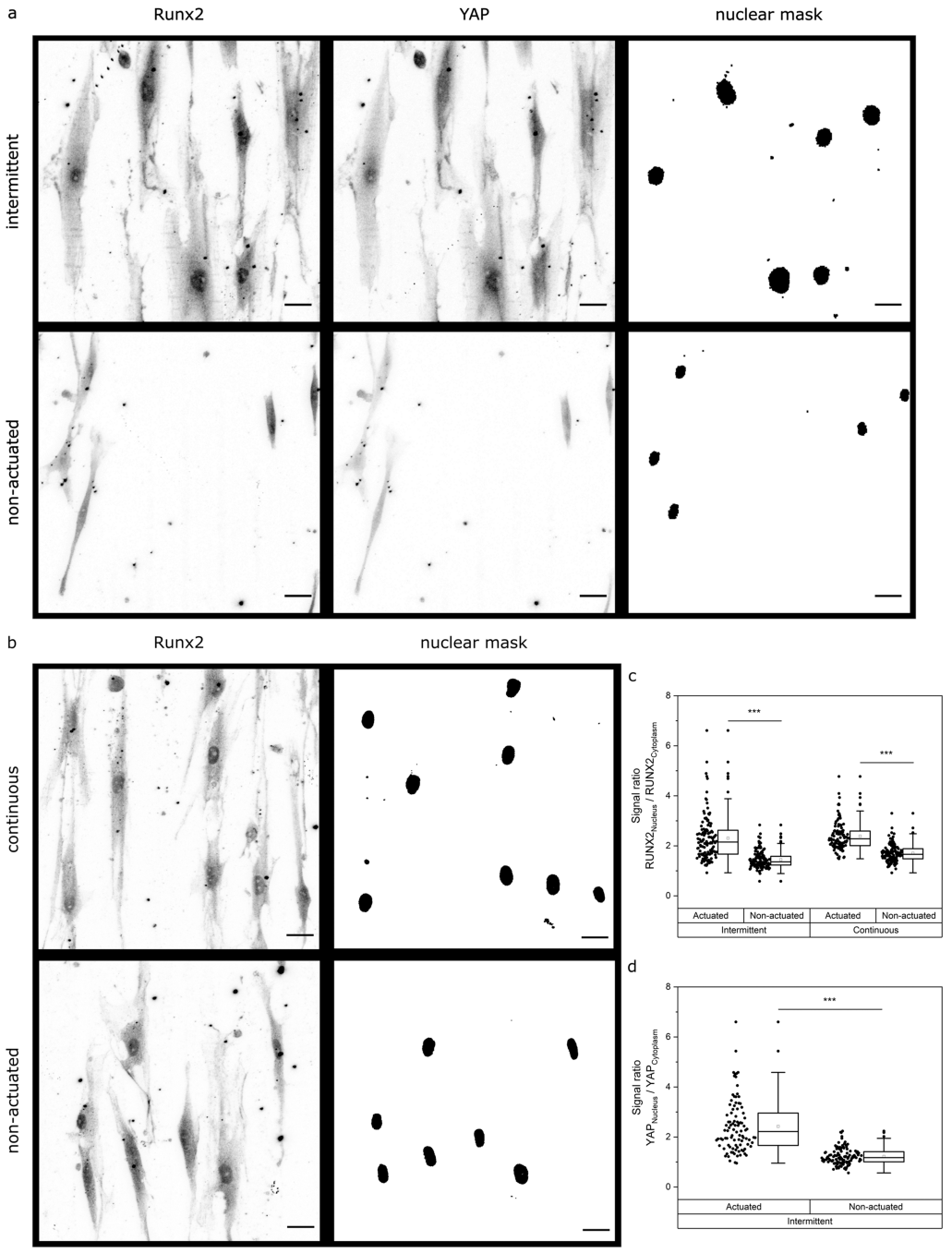

Figure 4. Actuation of MSCs on NIPAM/NEAM hydrogels increases nuclear translocation of Runx2 and YAP compared to nonactuated cells. (a) Immunofluorescence images showing the distribution of Runx2 and YAP in intermittently actuated and nonactuated MSCs. The determined mask of the nucleus is displayed on the right. (b) Immunofluorescence images showing the distribution of Runx2 inside continuously actuated MSCs. The determined mask of the nucleus is displayed on the right. (c) Quantification of the Runx2 nuclear/cytoplasmic signal ratio. Box plots show n = 3, $N \geq 115$ cells. (d) Quantification of the YAP nuclear/cytoplasmic signal ratio. Box plots show n = 2, $N \geq 95$ cells. In the box plots, the interquartile range (IQR) between the first and the third quartiles is indicated by the box, while whiskers denote 1.5 IQR. The hollow square, the horizontal line, and the filled dots represent the average, the median, and the outliers, respectively. *** is determined using a Mann−Whitney test and represents statistical significance at $p < 0.001$. Scale bar = 20 μm. MSC: Mesenchymal stem cell, NIPAM: *N*-isopropyl acrylamide, NEAM: *N*-ethyl acrylamide, Runx2: Runt-related transcription factor 2, YAP: Yes-associated protein.

YAP could also be affected by these mechanical stimuli provided by the dynamic hydrogel actuation. Nuclear localization of this transcriptional coregulator plays a major role in mediating mechanotransduction processes and is associated with osteogenesis of MSCs in 2D cultures, for example, triggered by stiffness, topography,[45] roughness,[46] ligand type, and ligand density.[47] To confirm this premise, the group of MSCs exposed to intermittent actuation, which shows the highest $Runx2_{nucleus}/Runx2_{cytoplasm}$ signal ratio upon actuation, was evaluated for nuclear translocation of YAP. In this case, MSCs exposed to actuation exhibit a higher nuclear YAP localization as compared to cells that remain on static regions on the same hydrogel (Figure 4b). Quantitative results show that the mean $YAP_{nucleus}/YAP_{cytoplasm}$ signal ratio increases

https://doi.org/10.1021/acsami.3c11808
ACS Appl. Mater. Interfaces 2024, 16, 30−43

1.98-fold on intermittently actuated versus static MSCs [Figure 4d]. Together, these results indicate that mechanical stimulation by actuating soft hydrogels modulates MSC fate commitment through enhanced cell spreading and YAP and Runx2 nuclear translocation.

DISCUSSION

The present study combines a soft (elastic modulus ∼30 kPa) light-responsive hydrogel system with a ridge/groove topography that exerts mechanical forces on human bone-marrow-derived MSCs. The dynamic local stresses applied to the cells, whether continuously or intermittently over the course of 3 days, result in morphological changes of the cell and nucleus, accompanied by increased nuclear import of the transcriptional activator YAP and preosteoblastic marker Runx2.

MSCs hold a large promise for stem cell-based therapies and regenerative medicine due to their easy accessibility from numerous tissues, multipotentiality, as well as their functional plasticity.[48] However, different harvesting and culturing procedures result in a large data variability among different publications.[49] Therefore, the harvested cells in this study are assessed on the minimal criteria from the Mesenchymal and Tissue Stem Cell Committee of the ISCT:[49] (1) MSCs must adhere to tissue culture flasks and demonstrate a fibroblastoid morphology while maintained in standard cell culture conditions; (2) MSCs must express the surface antigens CD73, CD90, and CD105 and lack expression of CD34, CD45, CD11b or CD14, CD79α or CD19, and HLA Class II; (3) MSCs must differentiate into osteoblasts, adipocytes, and chondroblasts in vitro, when exposed to standard protocols. The MSCs described here show the typical morphology, the correct markers, and the ability to differentiate into the desired mature cell types, improving the reproducibility of the results in this study.

One of the various applications for MSCs is transplantation into patients with large bone defects, for example, due to the removal of tumors or infected bone. Currently, an autologous bone graft is the gold standard, but this approach results in donor site morbidity and cannot always be performed.[50] Instead, the MSCs would be harvested relatively easily from the patient and differentiated into osteoblasts, which could be implanted together with a scaffold into the defect and accelerate and improve the healing process. To find an efficient and safe way to use MSCs in such therapies, it is important to understand what cues can guide MSC differentiation. Previous studies that focused on the effect of physical cues rather than biochemical cues showed that MSC differentiation in vitro can be triggered by various physical factors, such as topography[40] and stiffness[16] of the biomaterial, as well as cyclic stretching of the substrate.[51] Various systems have been used to stretch MSCs, including the Flexcell system (PDMS substrate),[38,52] ElectroForce 5210 BioDynamic-Test-System (combined with collagen-I sheets),[51,53] and multiple custom systems that stretch materials such as electrospun polycaprolactone scaffolds.[54] Most of these studies have shown that on a stiff substrate, cyclic stretch steers MSC differentiation into the direction of osteogenesis[52] and has a synergistic effect when used in combination with the osteogenic medium.[38] Importantly, most PDMS-based systems are limited to high stiffness. Therefore, softer systems are required to uncover mechanisms that might not be found when stiffer substrates. For example, one study has shown that cyclic stretch (1 Hz for 1 h) applied to MSCs cultured on a low stiffness collagen type I substrate (elastic modulus: 10 kPa) steers their differentiation into myogenic lineage.[51] Our hydrogel system has a stiffness of ∼30 kPa and is therefore softer compared to conventional PDMS-based systems. However, based on the hydrogel stiffness range studied by Engler et al. (0.1−40 kPa), our hydrogel can be qualified as "osteogenic".[16] Yet, we would like to point out that a significant increase in cell size and nuclear translocation of Runt-related transcription factor 2 (Runx2) and Yes-associated protein (YAP) is observed due to hydrogel actuation when compared to nonactuated cells on the same hydrogel. This suggests that our system likely speeds up the differentiation process. Another similar system, a hydrogel-actuated integrated responsive system also based on the photothermal actuation of PNIPAM, applied force on MSCs but did not include results on MSC differentiation or effects on molecular pathways.[55] In that study, the cells attached to stiffer Norland 61 epoxy pillars embedded in a PNIPAM hydrogel, which was actuated from 31 °C (VPTT PNIPAM hydrogels: 32 °C in water; in media, the VPTT is significantly reduced) to bend the pillars. During that study, cells were only actuated for several seconds to prove the bending of the pillars, and actuation over several days was not explored. Other soft hydrogel systems can be deformed but not reversibly or only in a time scale from minutes[56] to hours[28] and not in (milli)seconds, which is more relevant to study processes like breathing, walking, or heart beating. The time scale, stiffness of the substrate, and addition or absence of differentiation factors are all important factors during actuation experiments. In our system, we actuate cells for days on soft hydrogels and decouple mechanical from biochemical signals by using a basal medium to understand the mechanobiology of MSCs. Further studies should focus on combining dynamic force application with biochemical signaling, which has been found to have a synergistic effect on MSC osteogenesis.[38]

On static gels, it is well-known that a substrate with a high stiffness induces osteogenesis in MSCs.[16] In this study, circularity and spreading area are investigated since they can be used as cellular tension and substrate stiffness indicators.[23] Upon mechanical stimulation, cellular circularity decreases in intermittently actuated cells, while the cell spreading area visibly and significantly increases for actuated MSCs in both intermittent and continuous actuation conditions versus nonactuated MSCs. The cellular circularity and spreading area are therefore more sensitive to dynamic substrate mechanics than the cellular alignment and aspect ratio. The intermittently actuated cells have both a higher spreading area and more protrusions, similar to MSCs exposed to increases in substrate stiffness,[57] where several reports have shown that MSCs exhibit a lower circularity and larger spreading area.[58] For this reason, it could be hypothesized that the expansive and compressive stresses (although deformation is only ∼14%) produced by the actuating hydrogel not only make MSCs read a stiffer microenvironment as previously shown for fibroblasts as well,[59] but also activate internal mechanosensitive features that could diverge cell fate.[60]

As dynamic actuation of MSCs has a significant effect on their morphology, we hypothesized that downstream, this would affect the translocation of transcriptional coactivator YAP and preosteoblast transcription factor Runx2 from the cytoplasm to the nucleus. YAP and Runx2 translocation is highly dependent on matrix stiffness and occurs when MSCs are grown on increasingly rigid elastic substrates[32,61,62] or rapidly relaxing viscoelastic hydrogels.[19] Yet, as recent studies

https://doi.org/10.1021/acsami.3c11808
ACS Appl. Mater. Interfaces 2024, 16, 30−43

have demonstrated, cyclic stretching on stiff PDMS and polycaprolactone substrates also enhances YAP nuclear localization and Runx2 expression in rat or bovine MSCs, even in general, nonosteogenic media.[38,54] After YAP enters the nucleus, it interacts with the transcriptional enhanced associate domain (TEAD) transcriptional factors and regulates MSC gene expression for cellular differentiation.[61] Apart from the interaction with the TEAD protein family, YAP also acts as a coregulator for other transcription factors that play a key role in osteogenesis, such as Runx2.[63] The close interaction between these proteins has been further correlated by showing that MSC osteogenic differentiation on rigid substrates is inhibited upon YAP knockdown, thus exemplifying that YAP is required for preosteoblastic differentiation of MSCs.[61]

Alongside a higher cell area, indeed a significantly higher ratio of nuclear Runx2 is observed in both intermittent and continuous actuation conditions compared to nonactuated cells. Therefore, MSCs do not only respond morphologically to actuation but also start the process of osteogenesis, even without the addition of differentiation factors. Interestingly, we detect a higher fold increase of Runx2 translocation for intermittent actuation than for continuous actuation in comparison to no actuation. This is accompanied by the observation that cells have a higher number of protrusions (lower circularity) in intermittently actuated cells, whereas this effect does not take place for continuous actuation. Perhaps this morphological difference hints at the involvement of different mechanotransduction pathways. Previous studies using a PDMS stretching device without the addition of differentiation factors have found that osteogenesis in rodent MSCs is promoted through the p38MAPK-osterix pathway during intermittent stretch (0.8% strain, 0.5 Hz, 30 min twice a day),[64] yet this pathway is not involved in osteogenesis during continuous oscillating stress (10% strain, 1 Hz, 48 h).[65] The lower increase in nuclear Runx2 for continuous compared to intermittent actuation is likely not due to an overloading effect, as this has not been observed in any previous studies on the osteogenesis of MSCs. On the contrary, one study found that increasing cyclic tensile strain magnitude and frequency increases the expression of osteogenic markers after 21 days in a 3D endochondral ossification model (in the presence of chondrogenic growth factor TGF-β3).[66] However, for chondrogenesis of MSCs/adipose-derived stem cells, continuous rather than intermittent stretch or compression can overload the cells and block differentiation.[39,67]

In this study, MSCs are cultured on a slightly softer hydrogel (elastic modulus ~30 kPa), compared to the stiffness range that was previously described to induce osteogenesis (2D hydrogels with elastic moduli of 40[16]−68[68] kPa). However, dynamic actuation of the gel still leads to the nuclear import of YAP and Runx2. Although the exact pathways underlying preosteoblastic differentiation of MSCs upon mechanical actuation are not clear, we suspect that nuclear deformation also plays a role. Deformation enlarges the nuclear pores, increasing the translocation of proteins, such as YAP, into the nucleus.[69] After actuation, we observed increased cellular spreading, which can cause nuclear deformation since the nucleus and cytoskeleton are connected. In nonactuated cells, spreading remains unchanged and the import and export of proteins through the nuclear pores remains low. It was already reported that the transfer of strain to the nucleus through the cytoskeleton is required for YAP translocation when MSCs are exposed to dynamic actuation induced by a custom microtensile device, applying 3% strain at 1 Hz.[54] Decreasing the actomyosin contractility in these cells with Y27632 (a Rho-associated protein kinase inhibitor) decreases the amount of nuclear prestain, which reduces how much the nucleus can deform when stretch is applied, thus decreasing YAP translocation. Inversely, the application of stretch may lead to remodeling of the cytoskeleton, and different actuation/rest parameters may affect cell contractility. Actuation might also increase actin polymerization and reduce actin depolymerization, resulting in more sequestered angiomotin family proteins, which would otherwise inhibit YAP translocation.[70] This is in agreement with the fact that our previous study revealed nuclear translocation of MRTFA in fibroblasts when actuated with this hydrogel system, suggesting an increase in F-actin formation.[33] Interestingly, in previous reports using this light-actuating hydrogel platform, it was shown that YAP was already mostly localized in the nucleus in nonactuated fibroblasts,[33] whereas it was mostly located in the cytoplasm in nonactuated myoblasts.[34] This suggests that the elastic modulus of ~30 kPa is sufficiently high to deform the nucleus and facilitate YAP translocation in these fibroblasts, whereas it is too low for MSCs and myoblasts under static conditions. How cells respond to forces is, therefore, cell type-specific, and further studies should elucidate what conditions are optimal for each cell type and each application.

Although the molecular pathways engaged in MSC response to intermittent and continuous stretch might be different, the effect on osteogenic differentiation in short-term experiments was found to be similar.[64,65] During continuous stress, the peak of Runx2 expression (both on mRNA and protein level) was observed at 6 h. After 24 h, a higher expression of osteogenic markers alkaline phosphatase and collagen type I was found,[65] as was similarly seen for intermittent stretch (0.8% 0.5 Hz applied twice a day for 30 min).[64] However, these two studies used different strain amplitudes (0.8% and 10%) and frequencies (0.5 and 1 Hz). Therefore, via a more systematic approach, future research should clarify if intermittent and continuous stretching indeed has the same effect on the osteogenesis of MSCs and which mechanotransduction pathways are involved.

CONCLUSIONS

We report the use of a soft, light-responsive hydrogel with a ridge topography to mechanically stimulate MSCs through continuous (24 h actuation per day) or intermittent (12 h actuation/12 h rest per day) actuation for 3 days. Actuated cells show a higher spreading area and, for intermittently actuated cells, also higher protrusions, which is accompanied by increased nuclear import of the preosteoblastic marker Runx2 and the transcriptional activator YAP. We show for the first time with our soft, light-responsive dynamic hydrogel system that we can apply dynamic actuation and steer human MSC differentiation in the direction of osteogenesis in basal medium without the presence of biochemical differentiation factors. These results suggest that the actuation of MSCs on soft substrates can be used in the future to direct differentiation mechanically. An interesting opportunity for further research would be to investigate whether the addition of biochemical signals to this system could have synergistic effects on the osteogenesis of MSCs. These insights will improve our understanding of the mechanisms that regulate MSC behavior, which is important for improving the current and future applications of MSCs.

https://doi.org/10.1021/acsami.3c11808
ACS Appl. Mater. Interfaces 2024, 16, 30−43

■ ASSOCIATED CONTENT

Supporting Information

The Supporting Information is available free of charge at https://pubs.acs.org/doi/10.1021/acsami.3c11808.

Flow cytometry gate, differentiation potential of all three donors in standardized conditions (PDF)
NIPAM/NEAM hydrogel actuation (AVI)

■ AUTHOR INFORMATION

Corresponding Authors

Sabine Neuss − *Helmholtz Institute for Biomedical Engineering, BioInterface Group, RWTH Aachen University, Aachen D-52074, Germany; Institute of Pathology, RWTH Aachen University Hospital, Aachen D-52074, Germany*; Email: sneuss-stein@ukaachen.de

Laura De Laporte − *DWI—Leibniz Institute for Interactive Materials, Aachen D-52074, Germany; Institute for Technical and Macromolecular Chemistry, RWTH Aachen University, Aachen D-52074, Germany; Institute of Applied Medical Engineering, Department of Advanced Materials for Biomedicine, RWTH Aachen University, Aachen D-52074, Germany*; orcid.org/0000-0002-9438-0977; Email: delaporte@dwi.rwth-aachen.de

Authors

Arturo Castro Nava − *DWI—Leibniz Institute for Interactive Materials, Aachen D-52074, Germany; Institute for Technical and Macromolecular Chemistry, RWTH Aachen University, Aachen D-52074, Germany*

Iris C. Doolaar − *DWI—Leibniz Institute for Interactive Materials, Aachen D-52074, Germany; Institute for Technical and Macromolecular Chemistry, RWTH Aachen University, Aachen D-52074, Germany*

Norina Labude-Weber − *Helmholtz Institute for Biomedical Engineering, BioInterface Group, RWTH Aachen University, Aachen D-52074, Germany*

Hanna Malyaran − *Helmholtz Institute for Biomedical Engineering, BioInterface Group, RWTH Aachen University, Aachen D-52074, Germany; Interdisciplinary Centre for Clinical Research, RWTH Aachen University, Aachen D-52074, Germany*

Susan Babu − *DWI—Leibniz Institute for Interactive Materials, Aachen D-52074, Germany; Institute for Technical and Macromolecular Chemistry, RWTH Aachen University, Aachen D-52074, Germany*

Yashoda Chandorkar − *DWI—Leibniz Institute for Interactive Materials, Aachen D-52074, Germany;* Present Address: Laboratory for Biointerfaces, Empa, Swiss Federal Laboratories for Materials Science and Technology, St Gallen 9014, Switzerland

Jacopo Di Russo − *DWI—Leibniz Institute for Interactive Materials, Aachen D-52074, Germany; Interdisciplinary Centre for Clinical Research and Institute of Molecular and Cellular Anatomy, RWTH Aachen University, Aachen D-52074, Germany*

Complete contact information is available at: https://pubs.acs.org/10.1021/acsami.3c11808

Author Contributions

A.C.N.: methodology, investigation, validation, formal analysis, writing-original draft, and writing-review and editing; I.C.D.: writing-review and editing, visualization; N.L.-W.: investigation, formal analysis, and writing-review and editing; H.M.: investigation and writing-review and editing; S.B.: visualization and writing-review and editing; Y.C.: methodology, investigation, and writing-review and editing, funding acquisition; J.D.R.: conceptualization and writing-review and editing; S.N.: conceptualization, supervision, and writing-review and editing; L.D.L.: conceptualization, supervision, and writing-review and editing; A.C.N and I.C.D. contributed equally to this paper.

Notes

The authors declare no competing financial interest.

■ ACKNOWLEDGMENTS

The authors would like to acknowledge Dr. Rostislav Vinokur for support with electronic programming of the laser. We would also like to thank Céline Bastard for preparing hydrogels for some experiments. A. Castro Nava was funded by the Excellence Initiative of the German federal and state governments (project OPSF505) as well as the European Union's Horizon 2020 research and innovation program under the Marie Skłodowska-Curie grant agreement No 642687. I.C. Doolaar was funded by the Deutsche Forschungsgemeinschaft (DFG, German Research Foundation)—LA 3606/2-2. A.C.N., I.C.D., S.B., and Y.C. were supported by the Deutsche Forschungsgemeinschaft (DFG, German Research Foundation)—363055819/GRK2415. N.L.-W. and H.M. were funded by DFG Project NE1650/5-2 and IZKF Project OC1-3, respectively. S.B. was supported by the Max Planck School Matter to Life supported by the German Federal Ministry of Education and Research (BMBF) in collaboration with the Max Planck Society. J.D.R. was supported by a grant from the Interdisciplinary Centre for Clinical Research within the Faculty of Medicine at the RWTH Aachen University. S.N. was funded by an intramural position. L.D.L. was funded by the Leibniz Senate Competition Committee (SAW) under the Professorinnenprogramm (SAW-2017-PB62: BioMat), as well as the European Research Council (ERC)—(HEARTBEAT, Grant Agreement No. 101043656).

■ ABBREVIATIONS

AIM: adipogenic induction medium
AMM: adipogenic maintenance medium
ANOVA: analysis of variance
AR: aspect ratio
AuNR: gold nanorod
C: circularity parameter
CD: cluster of differentiation
CIM: chondrogenic induction medium
ECM: extracellular matrix
ISCT: International Society for Cellular Therapy
MAPK: mitogen-activated protein kinase
MRTFA: myocardin-related transcription factor A
MSC: mesenchymal stem cell
NEAM: *N*-ethyl acrylamide
NIPAM: *N*-isopropyl acrylamide
NIR: near-infrared
OIM: osteogenic induction medium
PDMS: polydimethylsiloxane
PEG: poly(ethylene glycol)
Runx2: Runt-related transcription factor 2
SCM: stem cell culture medium
TAZ: transcriptional coactivator with PDZ-binding motif
TCPS: tissue culture polystyrene

https://doi.org/10.1021/acsami.3c11808
ACS Appl. Mater. Interfaces 2024, 16, 30−43

TEAD: transcriptional enhanced associate domain
VPTT: volume phase transition temperature
YAP: Yes-associated protein
θ: orientation angle

REFERENCES

(1) Uccelli, A.; Moretta, L.; Pistoia, V. Mesenchymal Stem Cells in Health and Disease. *Nat. Rev. Immunol.* **2008**, *8* (9), 726−736.
(2) Stoeve, J.; Kern, S.; Bieback, K.; Klüter, H.; Eichler, H. Comparative Analysis of Mesenchymal Stem Cells from Bone Marrow, Umbilical Cord Blood, or Adipose Tissue. *Stem Cells* **2006**, *24* (5), 1294−1301.
(3) Friedenstein, A. J.; Petrakova, K. V.; Kurolesova, A. I.; Frolova, G. P. Heterotopic Transplants of Bone Marrow. *Transplantation* **1968**, *6* (2), 230−247.
(4) Zuk, P. A.; Zhu, M.; Ashjian, P.; De Ugarte, D. A.; Huang, J. I.; Mizuno, H.; Alfonso, Z. C.; Fraser, J. K.; Hedrick, M. H. Human Adipose Tissue Is a Source of Multipotent Stem Cells. *Mol. Biol. Cell* **2002**, *13* (12), 4279−4295.
(5) Ventura Ferreira, M. S.; Bienert, M.; Müller, K.; Rath, B.; Goecke, T.; Opländer, C.; Braunschweig, T.; Mela, P.; Brümmendorf, T. H.; Beier, F.; Neuss, S. Comprehensive Characterization of Chorionic Villi-Derived Mesenchymal Stromal Cells from Human Placenta. *Stem Cell Res. Ther.* **2018**, *9* (1), 1−17.
(6) Wang, H.-S.; Hung, S.-C.; Peng, S.-T.; Huang, C.-C.; Wei, H.-M.; Guo, Y.-J.; Fu, Y.-S.; Lai, M.-C.; Chen, C.-C. Mesenchymal Stem Cells in the Wharton's Jelly of the Human Umbilical Cord. *Stem Cells* **2004**, *22* (7), 1330−1337.
(7) Muguruma, Y.; Yahata, T.; Miyatake, H.; Sato, T.; Uno, T.; Itoh, J.; Kato, S.; Ito, M.; Hotta, T.; Ando, K. Reconstitution of the Functional Human Hematopoietic Microenvironment Derived from Human Mesenchymal Stem Cells in the Murine Bone Marrow Compartment. *Blood* **2006**, *107* (5), 1878−1887.
(8) Corcione, A.; Benvenuto, F.; Ferretti, E.; Giunti, D.; Cappiello, V.; Cazzanti, F.; Risso, M.; Gualandi, F.; Mancardi, G. L.; Pistoia, V.; Uccelli, A. Human Mesenchymal Stem Cells Modulate B-Cell Functions. *Blood* **2006**, *107* (1), 367−372.
(9) Spaggiari, G. M.; Capobianco, A.; Becchetti, S.; Mingari, M. C.; Moretta, L. Mesenchymal Stem Cell-Natural Killer Cell Interactions: Evidence That Activated NK Cells Are Capable of Killing MSCs, Whereas MSCs Can Inhibit IL-2-Induced NK-Cell Proliferation. *Blood* **2006**, *107* (4), 1484−1490.
(10) Wu, Y.; Chen, L.; Scott, P. G.; Tredget, E. E. Mesenchymal Stem Cells Enhance Wound Healing Through Differentiation and Angiogenesis. *Stem Cells* **2007**, *25* (10), 2648−2659.
(11) Pittenger, M. F.; Mackay, A. M.; Beck, S. C.; Jaiswal, R. K.; Douglas, R.; Mosca, J. D.; Moorman, M. A.; Simonetti, D. W.; Craig, S.; Marshak, D. R. Multilineage Potential of Adult Human Mesenchymal Stem Cells. *Science* **1999**, *284* (5411), 143−147.
(12) Petersen, B. E.; Bowen, W. C.; Patrene, K. D.; Mars, W. M.; Sullivan, A. K.; Murase, N.; Boggs, S. S.; Greenberger, J. S.; Goff, J. P. Bone Marrow as a Potential Source of Hepatic Oval Cells. *Science* **1999**, *284* (5417), 1168−1170.
(13) Jiang, Y.; Jahagirdar, B. N.; Reinhardt, R. L.; Schwartz, R. E.; Keene, C. D.; Ortiz-Gonzalez, X. R.; Reyes, M.; Lenvik, T.; Lund, T.; Blackstad, M.; Du, J.; Aldrich, S.; Lisberg, A.; Low, W. C.; Lergaespada, D. A.; Verfaillie, C. M. Pluripotency of Mesenchymal Stem Cells Derived from Adult Marrow. *Nature* **2002**, *418* (6893), 41−49.
(14) Bianco, P.; Cao, X.; Frenette, P. S.; Mao, J. J.; Robey, P. G.; Simmons, P. J.; Wang, C. Y. The Meaning, the Sense and the Significance: Translating the Science of Mesenchymal Stem Cells into Medicine. *Nat. Med.* **2013**, *19* (1), 35−42.
(15) Hajimiri, M.; Shahverdi, S.; Kamalinia, G.; Dinarvand, R. Growth Factor Conjugation: Strategies and Applications. *J. Biomed. Mater. Res. - Part A* **2015**, *103* (2), 819−838.
(16) Engler, A. J.; Sen, S.; Sweeney, H. L.; Discher, D. E. Matrix Elasticity Directs Stem Cell Lineage Specification. *Cell* **2006**, *126* (4), 677−689.
(17) Goetzke, R.; Sechi, A.; De Laporte, L.; Neuss, S.; Wagner, W. Why the Impact of Mechanical Stimuli on Stem Cells Remains a Challenge. *Cell. Mol. Life Sci.* **2018**, *75* (18), 3297−3312.
(18) Winer, J. P.; Janmey, P. A.; McCormick, M. E.; Funaki, M. Bone Marrow-Derived Human Mesenchymal Stem Cells Become Quiescent on Soft Substrates but Remain Responsive to Chemical or Mechanical Stimuli. *Tissue Eng. Part A* **2009**, *15* (1), 147−154.
(19) Chaudhuri, O.; Gu, L.; Klumpers, D.; Darnell, M.; Bencherif, S. A.; Weaver, J. C.; Huebsch, N.; Lee, H.; Lippens, E.; Duda, G. N.; Mooney, D. J. Hydrogels with Tunable Stress Relaxation Regulate Stem Cell Fate and Activity. *Nat. Mater.* **2016**, *15* (3), 326−334.
(20) Das, R. K.; Gocheva, V.; Hammink, R.; Zouani, O. F.; Rowan, A. E. Stress-Stiffening-Mediated Stem-Cell Commitment Switch in Soft Responsive Hydrogels. *Nat. Mater.* **2016**, *15* (3), 318−325.
(21) Kilian, K. A.; Bugarija, B.; Lahn, B. T.; Mrksich, M. Geometric Cues for Directing the Differentiation of Mesenchymal Stem Cells. *Proc. Natl. Acad. Sci. U. S. A.* **2010**, *107* (11), 4872−4877.
(22) Oh, S.; Brammer, K. S.; Li, Y. S. J.; Teng, D.; Engler, A. J.; Chien, S.; Jin, S. Stem Cell Fate Dictated Solely by Altered Nanotube Dimension. *Proc. Natl. Acad. Sci. U. S. A.* **2009**, *106* (7), 2130−2135.
(23) McBeath, R.; Pirone, D. M.; Nelson, C. M.; Bhadriraju, K.; Chen, C. S. Cell Shape, Cytoskeletal Tension, and RhoA Regulate Stem Cell Lineage Commitment. *Dev. Cell* **2004**, *6* (4), 483−495.
(24) Egusa, H.; Kobayashi, M.; Matsumoto, T.; Sasaki, J. I.; Uraguchi, S.; Yatani, H. Application of Cyclic Strain for Accelerated Skeletal Myogenic Differentiation of Mouse Bone Marrow-Derived Mesenchymal Stromal Cells with Cell Alignment. *Tissue Eng. - Part A* **2013**, *19* (5−6), 770−782.
(25) Simmons, C. A.; Matlis, S.; Thornton, A. J.; Chen, S.; Wang, C. Y.; Mooney, D. J. Cyclic Strain Enhances Matrix Mineralization by Adult Human Mesenchymal Stem Cells via the Extracellular Signal-Regulated Kinase (ERK1/2) Signaling Pathway. *J. Biomech.* **2003**, *36* (8), 1087−1096.
(26) Thiele, J.; Ma, Y.; Bruekers, S. M. C.; Ma, S.; Huck, W. T. S. 25th Anniversary Article: Designer Hydrogels for Cell Cultures: A Materials Selection Guide. *Adv. Mater.* **2014**, *26* (1), 125−148.
(27) Lee, T. T.; García, J. R.; Paez, J. I.; Singh, A.; Phelps, E. A.; Weis, S.; Shafiq, Z.; Shekaran, A.; del Campo, A.; García, A. J. Light-Triggered in Vivo Activation of Adhesive Peptides Regulates Cell Adhesion, Inflammation and Vascularization of Biomaterials. *Nat. Mater.* **2015**, *14* (3), 352−360.
(28) Rammensee, S.; Kang, M. S.; Georgiou, K.; Kumar, S.; Schaffer, D. V. Dynamics of Mechanosensitive Neural Stem Cell Differentiation. *Stem Cells* **2017**, *35* (2), 497−506.
(29) Lin, D. C.; Yurke, B.; Langrana, N. A. Mechanical Properties of a Reversible, DNA-Crosslinked Polyacrylamide Hydrogel. *J. Biomech. Eng.* **2004**, *126* (1), 104−110.
(30) Hörner, M.; Raute, K.; Hummel, B.; Madl, J.; Creusen, G.; Thomas, O. S.; Christen, E. H.; Hotz, N.; Gübeli, R. J.; Engesser, R.; Rebmann, B.; Lauer, J.; Rolauffs, B.; Timmer, J.; Schamel, W. W. A.; Pruszak, J.; Römer, W.; Zurbriggen, M. D.; Friedrich, C.; Walther, A.; Minguet, S.; Sawarkar, R.; Weber, W. Phytochrome-Based Extracellular Matrix with Reversibly Tunable Mechanical Properties. *Adv. Mater.* **2019**, *31* (12), No. 1806727.
(31) Lee, S.; Tong, X.; Yang, F. The Effects of Varying Poly(Ethylene Glycol) Hydrogel Crosslinking Density and the Crosslinking Mechanism on Protein Accumulation in Three-Dimensional Hydrogels. *Acta Biomater.* **2014**, *10* (10), 4167−4174.
(32) Yang, C.; Tibbitt, M. W.; Basta, L.; Anseth, K. S. Mechanical Memory and Dosing Influence Stem Cell Fate. *Nat. Mater.* **2014**, *13* (6), 645−652.
(33) Chandorkar, Y.; Castro Nava, A.; Schweizerhof, S.; Van Dongen, M.; Haraszti, T.; Köhler, J.; Zhang, H.; Windoffer, R.; Mourran, A.; Möller, M.; De Laporte, L. Cellular Responses to Beating Hydrogels to Investigate Mechanotransduction. *Nat. Commun.* **2019**, *10* (1), 1−13.

https://doi.org/10.1021/acsami.3c11808
ACS Appl. Mater. Interfaces 2024, 16, 30−43

(34) Chandorkar, Y.; Bastard, C.; Di Russo, J.; Haraszti, T.; De Laporte, L. Cells Feel the Beat − Temporal Effect of Cyclic Mechanical Actuation on Muscle Cells. *Appl. Mater. Today* **2022**, *27*, No. 101492.
(35) Haynesworth, S. E.; Goshima, J.; Goldberg, V. M.; Caplan, A. I. Characterization of Cells with Osteogenic Potential from Human Marrow. *Bone* **1992**, *13* (1), 81−88.
(36) Al Enezy-Ulbrich, M. A.; Malyaran, H.; de Lange, R. D.; Labude, N.; Plum, R.; Rütten, S.; Terefenko, N.; Wein, S.; Neuss, S.; Pich, A. Impact of Reactive Amphiphilic Copolymers on Mechanical Properties and Cell Responses of Fibrin-Based Hydrogels. *Adv. Funct. Mater.* **2020**, *30* (38), 1−11.
(37) Neuss, S.; Stainforth, R.; Salber, J.; Schenck, P.; Bovi, M.; Knüchel, R.; Perez-Bouza, A. Long-Term Survival and Bipotent Terminal Differentiation of Human Mesenchymal Stem Cells (HMSC) in Combination with a Commercially Available Three-Dimensional Collagen Scaffold. *Cell Transplant.* **2008**, *17* (8), 977−986.
(38) Li, R.; Liang, L.; Dou, Y.; Huang, Z.; Mo, H.; Wang, Y.; Yu, B. Mechanical Strain Regulates Osteogenic and Adipogenic Differentiation of Bone Marrow Mesenchymal Stem Cells. *Biomed Res. Int.* **2015**, *2015*, No. 873251.
(39) Horner, C. B.; Hirota, K.; Liu, J.; Maldonado, M.; Hyle Park, B.; Nam, J. Magnitude-dependent and Inversely-related Osteogenic/Chondrogenic Differentiation of Human Mesenchymal Stem Cells under Dynamic Compressive Strain. *J. Tissue Eng. Regen. Med.* **2018**, *12* (2), e637−e647.
(40) Abagnale, G.; Steger, M.; Nguyen, V. H.; Hersch, N.; Sechi, A.; Joussen, S.; Denecke, B.; Merkel, R.; Hoffmann, B.; Dreser, A.; Schnakenberg, U.; Gillner, A.; Wagner, W. Surface Topography Enhances Differentiation of Mesenchymal Stem Cells towards Osteogenic and Adipogenic Lineages. *Biomaterials* **2015**, *61*, 316−326.
(41) Caille, N.; Thoumine, O.; Tardy, Y.; Meister, J. J. Contribution of the Nucleus to the Mechanical Properties of Endothelial Cells. *J. Biomech.* **2002**, *35* (2), 177−187.
(42) Lee, J.; Abdeen, A. A.; Kilian, K. A. Rewiring Mesenchymal Stem Cell Lineage Specification by Switching the Biophysical Microenvironment. *Sci. Rep.* **2014**, *4*, 20−27.
(43) James, A. W. Review of Signaling Pathways Governing MSC Osteogenic and Adipogenic Differentiation. *Scientifica (Cairo).* **2013**, *2013*, 1−17.
(44) Bruderer, M.; Richards, R. G.; Alini, M.; Stoddart, M. J. Role and Regulation of Runx2 in Osteogenesis. *Eur. Cells Mater.* **2014**, *28*, 269−286.
(45) Omidinia-Anarkoli, A.; Rimal, R.; Chandorkar, Y.; Gehlen, D. B.; Rose, J. C.; Rahimi, K.; Haraszti, T.; De Laporte, L. Solvent-Induced Nanotopographies of Single Microfibers Regulate Cell Mechanotransduction. *ACS Appl. Mater. Interfaces* **2019**, *11* (8), 7671−7685.
(46) Faia-Torres, A. B.; Charnley, M.; Goren, T.; Guimond-Lischer, S.; Rottmar, M.; Maniura-Weber, K.; Spencer, N. D.; Reis, R. L.; Textor, M.; Neves, N. M. Osteogenic Differentiation of Human Mesenchymal Stem Cells in the Absence of Osteogenic Supplements: A Surface-Roughness Gradient Study. *Acta Biomater.* **2015**, *28*, 64−75.
(47) Stanton, A. E.; Tong, X.; Yang, F. Extracellular Matrix Type Modulates Mechanotransduction of Stem Cells. *Acta Biomater.* **2019**, *96* (June), 310−320.
(48) Horwitz, E. M.; Gordon, P. L.; Koo, W. K. K.; Marx, J. C.; Neel, M. D.; McNall, R. Y.; Muul, L.; Hofmann, T. Isolated Allogeneic Bone Marrow-Derived Mesenchymal Cells Engraft and Stimulate Growth in Children with Osteogenesis Imperfecta: Implications for Cell Therapy of Bone. *Proc. Natl. Acad. Sci. U. S. A.* **2002**, *99* (13), 8932−8937.
(49) Dominici, M.; Le Blanc, K.; Mueller, I.; Slaper-Cortenbach, I.; Marini, F.; Krause, D. S.; Deans, R. J.; Keating, A.; Prockop, D. J.; Horwitz, E. M. Minimal Criteria for Defining Multipotent Mesenchymal Stromal Cells. The International Society for Cellular Therapy Position Statement. *Cytotherapy* **2006**, *8* (4), 315−317.
(50) Stanovici, J.; Le Nail, L. R.; Brennan, M. A.; Vidal, L.; Trichet, V.; Rosset, P.; Layrolle, P. Bone Regeneration Strategies with Bone Marrow Stromal Cells in Orthopaedic Surgery. *Curr. Res. Transl. Med.* **2016**, *64* (2), 83−90.
(51) Rothdiener, M.; Hegemann, M.; Uynuk-Ool, T.; Walters, B.; Papugy, P.; Nguyen, P.; Claus, V.; Seeger, T.; Stoeckle, U.; Boehme, K. A.; Aicher, W. K.; Stegemann, J. P.; Hart, M. L.; Kurz, B.; Klein, G.; Rolauffs, B. Stretching Human Mesenchymal Stromal Cells on Stiffness-Customized Collagen Type I Generates a Smooth Muscle Marker Profile without Growth Factor Addition. *Sci. Rep.* **2016**, *6*, 35840.
(52) Wang, J.; Wang, C. D.; Zhang, N.; Tong, W. X.; Zhang, Y. F.; Shan, S. Z.; Zhang, X. L.; Li, Q. F. Mechanical Stimulation Orchestrates the Osteogenic Differentiation of Human Bone Marrow Stromal Cells by Regulating HDAC1. *Cell Death Dis.* **2016**, *7*, No. e2221.
(53) Walters, B.; Uynuk-Ool, T.; Rothdiener, M.; Palm, J.; Hart, M. L.; Stegemann, J. P.; Rolauffs, B. Engineering the Geometrical Shape of Mesenchymal Stromal Cells through Defined Cyclic Stretch Regimens. *Sci. Rep.* **2017**, *7* (1), 6640.
(54) Driscoll, T. P.; Cosgrove, B. D.; Heo, S. J.; Shurden, Z. E.; Mauck, R. L. Cytoskeletal to Nuclear Strain Transfer Regulates YAP Signaling in Mesenchymal Stem Cells. *Biophys. J.* **2015**, *108* (12), 2783−2793.
(55) Sutton, A.; Shirman, T.; Timonen, J. V. I.; England, G. T.; Kim, P.; Kolle, M.; Ferrante, T.; Zarzar, L. D.; Strong, E.; Aizenberg, J. Photothermally Triggered Actuation of Hybrid Materials as a New Platform for in Vitro Cell Manipulation. *Nat. Commun.* **2017**, *8* (1), 14700.
(56) Rosales, A. M.; Mabry, K. M.; Nehls, E. M.; Anseth, K. S. Photoresponsive Elastic Properties of Azobenzene-Containing Poly-(Ethylene-Glycol)-Based Hydrogels. *Biomacromolecules* **2015**, *16* (3), 798−806.
(57) Galarza Torre, A.; Shaw, J. E.; Wood, A.; Gilbert, H. T. J.; Dobre, O.; Genever, P.; Brennan, K.; Richardson, S. M.; Swift, J. An Immortalised Mesenchymal Stem Cell Line Maintains Mechano-Responsive Behaviour and Can Be Used as a Reporter of Substrate Stiffness. *Sci. Rep.* **2018**, *8* (1), 1−13.
(58) Gerardo, H.; Lima, A.; Carvalho, J.; Ramos, J. R. D.; Couceiro, S.; Travasso, R. D. M.; Pires Das Neves, R.; Grãos, M. Soft Culture Substrates Favor Stem-like Cellular Phenotype and Facilitate Reprogramming of Human Mesenchymal Stem/Stromal Cells (HMSCs) through Mechanotransduction. *Sci. Rep.* **2019**, *9* (1), 9086.
(59) Cui, Y.; Hameed, F. M.; Yang, B.; Lee, K.; Pan, C. Q.; Park, S.; Sheetz, M. Cyclic Stretching of Soft Substrates Induces Spreading and Growth. *Nat. Commun.* **2015**, *6*, 1−8.
(60) Treiser, M. D.; Yang, E. H.; Gordonov, S.; Cohen, D. M.; Androulakis, I. P.; Kohn, J.; Chen, C. S.; Moghe, P. V. Cytoskeleton-Based Forecasting of Stem Cell Lineage Fates. *Proc. Natl. Acad. Sci. U. S. A.* **2010**, *107* (2), 610−615.
(61) Dupont, S.; Morsut, L.; Aragona, M.; Enzo, E.; Giulitti, S.; Cordenonsi, M.; Zanconato, F.; Le Digabel, J.; Forcato, M.; Bicciato, S.; Elvassore, N.; Piccolo, S. Role of YAP/TAZ in Mechanotransduction. *Nature* **2011**, *474* (7350), 179−183.
(62) Ducy, P.; Zhang, R.; Geoffroy, V.; Ridall, A. L.; Karsenty, G. Osf2/Cbfa1: A Transcriptional Activator of Osteoblast Differentiation. *Cell* **1997**, *89* (5), 747−754.
(63) Pan, J. X.; Xiong, L.; Zhao, K.; Zeng, P.; Wang, B.; Tang, F. L.; Sun, D.; Guo, H. H.; Yang, X.; Cui, S.; Xia, W. F.; Mei, L.; Xiong, W. C. YAP Promotes Osteogenesis and Suppresses Adipogenic Differentiation by Regulating β-Catenin Signaling. *Bone Res.* **2018**, *6* (1), 1−12.
(64) Xiao, W. L.; Zhang, D. Z.; Fan, C. H.; Yu, B. J. Intermittent Stretching and Osteogenic Differentiation of Bone Marrow Derived Mesenchymal Stem Cells via the P38MAPK-Osterix Signaling Pathway. *Cell. Physiol. Biochem.* **2015**, *36* (3), 1015−1025.

https://doi.org/10.1021/acsami.3c11808
ACS Appl. Mater. Interfaces 2024, 16, 30−43

(65) Zhang, P.; Wu, Y.; Dai, Q.; Fang, B.; Jiang, L. P38-MAPK Signaling Pathway Is Not Involved in Osteogenic Differentiation during Early Response of Mesenchymal Stem Cells to Continuous Mechanical Strain. *Mol. Cell. Biochem.* **2013**, *378* (1−2), 19−28.
(66) Carroll, S. F.; Buckley, C. T.; Kelly, D. J. Cyclic Tensile Strain Can Play a Role in Directing Both Intramembranous and Endochondral Ossification of Mesenchymal Stem Cells. *Front. Bioeng. Biotechnol.* **2017**, *5* (NOV), 1−12.
(67) Tseng, S. J.; Wu, C. C.; Cheng, C. H.; Lin, J. C. Studies of Surface Grafted Collagen and Transforming Growth Factor B1 Combined with Cyclic Stretching as a Dual Chemical and Physical Stimuli Approach for Rat Adipose-Derived Stem Cells (RADSCs) Chondrogenesis Differentiation. *J. Mech. Behav. Biomed. Mater.* **2020**, *112* (April), No. 104062.
(68) Sun, M.; Chi, G.; Xu, J.; Tan, Y.; Xu, J.; Lv, S.; Xu, Z.; Xia, Y.; Li, L.; Li, Y. Extracellular Matrix Stiffness Controls Osteogenic Differentiation of Mesenchymal Stem Cells Mediated by Integrin A5. *Stem Cell Res. Ther.* **2018**, *9* (1), 1−13.
(69) Elosegui-Artola, A.; Andreu, I.; Beedle, A. E. M.; Lezamiz, A.; Uroz, M.; Kosmalska, A. J.; Oria, R.; Kechagia, J. Z.; Rico-Lastres, P.; Le Roux, A. L.; Shanahan, C. M.; Trepat, X.; Navajas, D.; Garcia-Manyes, S.; Roca-Cusachs, P. Force Triggers YAP Nuclear Entry by Regulating Transport across Nuclear Pores. *Cell* **2017**, *171* (6), 1397−1410.
(70) Kassianidou, E.; Kalita, J.; Lim, R. Y. H. The Role of Nucleocytoplasmic Transport in Mechanotransduction. *Exp. Cell Res.* **2019**, *377* (1−2), 86−93.

https://doi.org/10.1021/acsami.3c11808
ACS Appl. Mater. Interfaces 2024, 16, 30−43